SMALL SATELLITE DESIGN AND DEVELOPMENT FOR PRECISION POINTING APPLICATIONS

M. Socha, R. Hain, C. Dever. P. Madden, R. Mangoubi, R. Metzinger

The Charles Stark Draper Laboratory, Inc.
555 Technology Sq.
Cambridge, MA 02139
617.258.2126
msocha@draper.com

Abstract. The move towards miniaturizing satellites will not be based solely on scaling down with a commensurate reduction in capability. The real goal should be to maintain high functionality and ultimately to increase capability in a small, low cost package. Conventional remote imaging has been based on the design approach that to achieve high resolution images from space, the satellite designer is driven to large apertures, expensive and complex attitude and articulation control hardware, with large, heavy, and power intensive inertial sensors. Micro-class satellites when faced with precision pointing requirements have traditionally not used active control to improve pointing performance. This paper describes MicroSat, a three axis stabilized satellite design for precision pointing applications. The heart of the design is the optics and the pointing subsystems. MicroSat uses an integrated INS/GPS based attitude reference system with custom designed and fabricated reaction wheels for pointing control. Multiple units can be launched from a Pegasus class vehicle providing a once-per-day revisit of a designated area with one meter class resolution in the visible range. This paper describes the satellite concept design and the hardware ground test demonstration.

Introduction

Traditionally micro-class satellites have approached the pointing subsystem with passive pointing and control. A common approach has been for the satellite to be a free floating bus, using gravity gradients for attitude control. The MicroSat concept actively controls line-of-sight pointing and slewing by utilizing on-board attitude determination, inertial sensing, and closed-loop error correction with reaction wheel control actuators. This class of mission has traditionally been deemed too complicated or expensive for this size. Our approach is an integrated design wherein science, bus, and instrument are one and the same. Subsystems were traded to achieve low cost, low power, and reliable mission segments in a 50 kg package. To the question, "how much of the satellite is the payload?" the response is, "the satellite is the payload."

The cost and complexity of conducting space missions with individual, highly integrated, large satellites continue to escalate. To reduce costs, more effort and attention is being directed toward small, light-weight satellites where future demand is expected to grow dramatically. During the past few years significant effort has been made to develop new technologies in the design of microsatellites to prepare for space missions of the future. Recent advances in silicon microfabrication technology have led to the development of low cost micromechanical inertial sensors. The small size, minimized weight, and low cost attributes of these sensors permit on-board inclusion of gyroscopes and accelerometers for space applications previously considered impractical because of size and cost of traditional inertial sensors.

A micro-class spacecraft with a precision pointing requirement is a unique design challenge for the hardware, instrument, and payload designers. This class of satellite is an ideal application for micromechanical gyros to provide the inertial reference information needed to perform image motion compensation, stabilization and the reduction of image smear in an extremely small and light weight package.

Existing microsatellite pointing systems do not employ active control to improve pointing performance. Some systems allow the bus to point coarsely, then hope to get useful data by taking many images. GPS alone will not provide sufficient accuracy. However, line-of-sight pointing can be controlled by on-board attitude determination from micromechanical inertial sensors, coupled with GPS, and closed-loop rate error correction with slew control actuators. Others have not undertaken this approach since traditional inertial reference systems are significantly heavier and larger than the micromechanical package, and could consume a significant fraction of the mass budget for an entire micro-class satellite.

The concept described herein consists of a three axis stabilized system using on-board GPS, next-generation micromechanical inertial instruments, small reaction wheels for attitude control, and miniaturized phased array antennas for line-of-sight communications. The basic structure will be constructed with advanced

graphite-epoxy composite materials. Material fabrication is kept cost-effective by using simple shapes and optimizing the overall configuration. Body-fixed solar cells, as well as batteries, are used. This flexibility permits selection and adjustment of the center of gravity to be near-coincident with the center-of-pressure to minimize rotational torques due to atmospheric drag.

The feasibility of a micromechanical gyro to provide sufficient performance to accomplish a pointing mission has been analyzed for a bandwidth of 0.1 Hz, based on estimated external and induced disturbance frequencies. From a first-order simulation, it was determined that the performance of existing micromechanical gyros with integrated GPS is capable of providing pointing jitter stability better than 10 microradians and absolute pointing error of approximately 1 milliradian, for a satellite with 1 meter antenna separation (i.e., 1m baseline). This result is encouraging and gives credence to the overall concept and approach.

Mission Description

Sample missions for this class of microsatellite includes tactical and commercial science applications. The tactical reconnaissance mission would provide moderate resolution images to field commands in a timely manner. The proposed system would provide sufficient resolution to give a broad overview of current military assets. This data would be relayed directly to local field command via an encrypted downlink from the satellite. With high revisit frequency from one or more satellites, the data would reflect current conditions, or provide early warning of significant movement of assets. A single image could detect the movement of specific assets by use of shadow observing since the satellite will have constant solar lighting conditions on every pass.

Attitude knowledge assumes that the satellite will process GPS-derived attitude measurements (and perhaps attitude-rate) and gyro-derived attitude rate measurements while in orbit to establish estimates of gyro drift bias and scale factor (SF). Satellite maneuvers can be used to separate the error components due to bias and SF. Accelerometer measurements can be used to provide delta velocity in cases where the satellite may require orbit changes.

A typical pointing scenario is accomplished for every identified target. The satellite is pitched forward from a nominal nadir-pointing attitude to some new attitude, and then pitched in reverse during imaging to reduce the transverse velocity of the line-of-sight at the surface of the earth. Without this counter-motion, the satellite velocity over an integration period will result in too much blur of the picture. In order to satisfy this requirement, the additional drift (i.e., in addition to the nominal drift due to satellite motion) over an integration period should not exceed the equivalent of 1 pixel motion. The amount by which the satellite must be initially pitched forward in preparation for the imaging slew depends upon the amount of time required to settle out initial pitch slew transients once the imaging slew begins. The time requirement, in turn, depends upon the controller bandwidth. A higher controller bandwidth will result in transients subsiding quicker but will result in a greater response to sensor noise. A 0.03 Hz controller bandwidth requires an initial attitude of a least 60° of the nadir and a 0.1 Hz controller bandwidth requires less than 30°.

During this large angular rotation over a short period of time, there will likely be several changes of GPS satellites and possibly, a large variation of attitude precision. Therefore, attitude measurements from GPS will be effectively suppressed during the imaging slew and attitude inputs to the controller will rely essentially upon calibrated gyro measurements. Calibration of the gyros depends upon the effectiveness of the integrated GPS/gyro filter.

If gyro calibration is not sufficiently accurate, it may be necessary to pause at the end of the preparatory pitch-forward maneuver to regain the required absolute attitude accuracy by again processing GPS attitude measurements at the new pitch attitude. If this angle is large, a second set of GPS antennas might have to be used to obtain satisfactory satellite visibility. On the other hand, if the angle is small, as required for the 0.1 Hz controller, a single set of antennas may suffice for both the nadir and off-nadir satellite attitudes.

Orbit Design

Orbit design for the Microsat required compromise among several requirements:

• A low altitude to satisfy the 1 meter resolution optical requirement without large optics.

• A high altitude so that the 90 day mission duration requirement could be met without excessive fuel.

• A daily revisit requirement with consistent lighting conditions.

A class of orbits known as sun-synchronous repeat groundtrack orbits will satisfy the revisit and lighting constraints, but it remains to select one orbit from this class that will meet the duration and optical resolution requirements. Repeat ground track orbits are orbits in

2

which the ratio of the orbital nodal period and the period of rotation of the earth can be expressed as the ratio of two integers.

$$\frac{\text{Nodal Period}}{\text{Earth Period}} = \frac{M}{N}$$

The satellite makes M orbits in N days, and will pass over the same location on the earth every N days. The Nodal Period is a function of the satellite altitude or semi-major axis, so a selection of the M/N ratio will directly yield a choice for satellite altitude.

Sun-synchronous orbits are near polar orbits where the plane of the orbit precesses in inertial space at a rate of one revolution per year. The effect of this rotation is that the angle between the line of sight to the sun and the orbital plane remains constant. The result is constant solar lighting conditions to the satellite. The sun-synchronous condition is achieved by choosing, for a given altitude, an appropriate inclination such that the orbital perturbation caused by solar gravity results in the desired rate of change of the right ascension of the ascending node (0.9856 deg/day). The subclass of sun-synchronous repeat groundtrack orbits with a daily repeat cycle (N = 1) was examined using analytic equations that include the J2 and J3 perturbations to the earth's gravity potential. Various values of M were used. The resulting orbits where evaluated for compatibility with the altitude constraints and a down select made among the candidates for further design refinement. Initial analysis of the orbital elements was made using the Draper Semi-Analytic Satellite Theory (DSST) mean element orbit propagator [1]. This refinement step is essentially a "point" design in time but using all available orbital perturbations. Final refinement, evaluation and stability analyses were performed to study orbit evolution over the 90 day mission lifetime. Variations in atmospheric drag due to the sun spot cycle were evaluated over a six year period commencing in 1997 and ending in 2002.

Orbit stability was analyzed by studying the evolution of the orbit over time by integrating the refined element set for 90 days. The orbit was found to be stable with respect to perturbations introduced by Third Body Gravity (Lunar and Solar), Solar Radiation Pressure, and Zonal and Tesseral Harmonics. The most significant of all these perturbations was a secular increase in inclination caused by Third body (Solar) effects with a magnitude of about 200 micro-radians/year (0.0034 deg/yr).

At a mean height of 410 km, the satellite will be subject to considerable atmospheric drag. The effect varies with the sun-spot cycle. The orbit was again propagated using the Draper Semi-Analytic Orbit Generator with a Jacchia-Roberts atmospheric density model containing predicted parameters for the next solar cycle. Runs were made with "nominal predicted parameters" and with ± 2 sec parameters for a 90 day period in each of five years straddling the next peak in solar activity, with satellite mass of 50 kg, satellite area of 0.35 meters squared, and a drag coefficient of 2.0. The effect of drag shows a decrease in semi-major axis that occurs over a period of 35 days for a spacecraft launched on Jan. 1 of the relevant year. The worst case occurs in the year 2000 where 31.72 km are lost in the first 35 days. In actual spacecraft operation, drag makeup thrusting maneuvers will have to be performed to compensate for the drag and to maintain the nominal semi-major axis.

The design space for repeat mission groundtrack orbits with N = 1 is rather sparse. The only viable options are N/M = 15:1 and N/M = 16:1. Orbital elements for these options are provided below in Table 1.

Table 1. Orbit Elements for Sun Synchronous Daily Repeat Orbits

Orbit	Axis (km)	Alt. (km)	Inclin. (deg)	Ecc.	Arg. P (deg)
16:1	6653	274	96.5806	1.119E-3	± 90°
15:1	6945	566	97.6582	1.069E-3	± 90°

Neither of these two candidate orbits has an acceptable altitude. The 16:1 orbit is too low, and will encounter excessive atmospheric drag. The 15:1 orbit is too high and will require optics with an excessively large aperture. However, it is possible to meet the daily revisit requirement by using two satellites operating in the same orbit but separated by 180 degrees in mean anomaly. With this arrangement, a satellite will pass over the reference location every 24 hours.

The preliminary orbital elements were refined using Flight Dynamics software developed at Draper Laboratory. The refined orbit is sun synchronous and in addition has been designed so that the argument of perigee and the eccentricity are stable (Frozen Orbit). This means that when the satellite revisits a location, the height above the surface is the same as on previous visits.

ORBITAL PARAMETERS (Mean Elements)

Semi-major Axis	6788.780	km
Eccentricity	0.001262	N/A
Inclination	97.0902	
Ascending Node	190.0	Deg
Arg. of Perigee	90.0	Deg

3

Height at Apogee	419.20	km
Height at Perigee	402.07	km
Angle to Mean Sun	6	hrs
Repeat Cycle		
Orbits/cycle	31	orbits
Days/cycle	2	days
Epoch	Jan 1, 0000hrs UT	

Satellite Description

The MicroSat spacecraft is capable of meeting all design requirements while supporting mission operations throughout program life. The satellite is a custom design estimated to be 50 kg dry mass, diameter of 0.5 meter, and an overall length of 1 meter. To accomplish the mass goal, the bus structure, telescope housing, and electronics deck are made from advanced graphite-epoxy composite materials. This material is kept cost effective by designing simple shapes and optimizing the overall configuration. To minimize cost and increase reliability, no deployment mechanisms or articulated platforms are employed.

MicroSat is a three-axis stabilized structure that combines gyros for inertial reference, GPS for attitude determination, and small reaction wheels as control actuators. Spacecraft hardware consists of components with flight-proven heritage, state-of-the-practice technologies, and a lightweight structure for an optimized mass-to-bending stiffness.

MICROSAT

SOLAR CELLS
BATTERY
GYRO PACKAGE
TORQUE RODS (3)
REACTION WHEELS (3)
OPTICS ASSEMBLY
ELECTRONICS
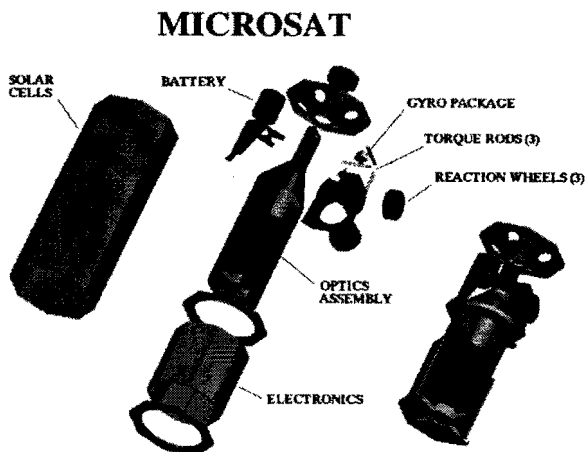
Preliminary configuration, analysis, and system trades have been completed, resulting in a mature design. Mass and power budgets and the key components have been prepared. The satellite has body fixed solar cells and secondary batteries for acquisition and eclipse. The primary optical receiver is a 37 centimeter mirror (for a 409 km altitude) with a line-array charge coupled device (CCD) for imaging. Electromagnetic torque rods provide momentum unloading. Communication will be body-fixed, high bandwidth phased array antennas. The satellite uses miniaturized antennas and assumes a line-of-sight communication view. Two methods of satellite communication were examined: radio based and laser based. The laser system may offer as advantages reduced supply power, higher bandwidth and the dual use of the telescope objective as an imager and a transmitter/receiver antenna, but may be too high a technical risk. A radio based concept would be more conventional and therefore was selected.

Requirements
Spacecraft requirements resulted from interactive matching of pointing requirements, mission operations, and operational constraints. The MicroSat spacecraft design satisfies the entire flow down of requirements from the payload while minimizing overall mass and power.

Attitude and Orbit Control
MicroSat is an inertially stabilized spacecraft using GPS and a three-axis inertial sensor as the primary attitude sensor. An integrated assembly of four small reaction wheels provides attitude control, with electromagnetic torque rods for momentum unloading. All systems are mounted directly to the spacecraft structure with no articulated platforms, gimbaled subsystems, or deployable solar panels. This arrangement requires the entire satellite to be pointed for science, communications, momentum unloading, and telescope protection. A preliminary covariance analysis has been performed assessing the IMU, and pointing requirements. Analysis indicates that adequate pointing knowledge, with margin, can be achieved and is described in detail in another section.

Power Generation
The electric power subsystem consists of body-fixed solar arrays, a power controller, and battery storage that provides electrical power to the satellite during all mission phases. Different modes of operation during the mission require different power levels. Peak power requirements are during imaging and communication with the ground station. The electrical power requirement for these modes is 125 W. The primary source of electric power are the solar arrays, which are attached to the outside of the structure with space-qualified silicone adhesive. They have been sized to provide adequate power with margin. Power for the satellite is provided by Super NiCd™ batteries for eclipse periods.

4

Structural

Structural design of the spacecraft comprises a primary structure capable of surviving launch loads, and providing adequate structural stiffness to eliminate controls/structure interaction during pointing maneuvers. Configuration trades resulted in an axisymmetric, octagonal shape. The structural system consists of lightweight honeycomb panels with a ring structure supporting the panels. The structural design for this configuration provides an adequate safety factor for strength and buckling under all launch and operational conditions while minimizing mass.

Command and Data Handling (C&DH)

The C&DH functions, which include satellite-to-ground communications, and satellite control, are accomplished in the computation and communication hub. The computation hub consists of an SWRI SC-9 RAD6000-based computer, error detecting and correcting memory, backplane, and all system and applications software. The communications hub receives instrument and satellite data directly from the computation hub for downlink transmission to the ground station via the X-band antenna system, and the uplink is accomplished through the omnidirectional S-band receiver. The bus architecture, which includes the MIL-STD-1553, is the communications link between the computation hub and the utility hub, power node, and IMU. The utility hub serves as interface and controller for thermistors, magnetic torquers, heaters, hydrazine thrusters. The data bus is also the communications channel between the computation hub and the integrated reaction wheel assembly. All key computation hub components are nondevelopmental items and space-qualified.

Communications

This subsystem is accomplished with body-fixed, high-bandwidth, phased-array antennas. The satellite assumes a line-of-sight communication link to a X-band antenna on the ground. The communications subsystem has been designed to provide a minimum 200MPS downlink.

Thermal

The thermal control subsystem is designed to maintain and measure all component temperatures within acceptable operating ranges. The thermal subsystem will accommodate seasonal changes over the mission life from changes in the sun angle. A combination of surface treatment, multilayer insulation, and component placement will be used to provide passive thermal control wherever possible, with backup heaters to supplement this approach, resulting in a semipassive thermal control subsystem.

Optical Design

Since the satellite's ground resolution performance is the key parameter to be optimized in the optical system, the performance metric employed is the Modulation Transfer Function (MTF) [4]. This metric is a measure of the contrast of an image at a given spatial frequency and wavelength. An MTF equal to one represents perfect contrast, an MTF equal to zero represents no contrast and hence no image information.

$$MTF = \frac{I_{bright} - I_{dark}}{I_{bright} + I_{dark}}$$

A good analogy is the viewing of a white picket fence against a dark background. If our eyesight is good, the pickets will form a sharply contrasting image on our retina, i.e., an MTF $\approx$ 1. The spatial frequency of the image is the number of pickets in a given distance on the retina. This is frequently expressed in units of line pairs per millimeter. The width of a picket plus the width of a space between two pickets being equal to one line pair. As we step away from the fence the spacing between the pickets on our retina gets smaller and consequently, the spatial frequency of their image gets larger. At some point as we keep stepping away, the image of the fence gets blurrier. The sharp square-wave intensity pattern of the fence becomes more sinusoidal and the difference between the bright intensity of the pickets and the darkness of the spaces diminishes. Eventually, all that we see of the fence is a gray, even brightness patch, i.e., an MTF $\approx$ 0.

The power of the MTF approach to image resolution quantification is that the degradation of all the error sources (optics, jitter, image motion, pixel size) can be quantified this way and their combined effect can be determined by multiplying the cascade of individual MTFs together to yield a total system MTF.

The polychromatic MTF calculation was performed for the specified telescope at three different field angles: on-axis and off-axis field angles corresponding to the edge corner of the same two candidate CCD's. At the sampling spatial frequency of 69 line-pairs per millimeter, the MTF design performance on-axis and at the smaller CCD corner edge is diffraction limited and about 0.36. We see that the performance at the larger CCD corner edge is low, this is due mostly to field curvature of the focal surface and astigmatism. It is apparent that the best focal position moves closer to the telescope mirrors as the field angle increases.

The field angle dependent image defects of the telescope are correctable using a weak negative meniscus lens in-front of the CCD. A field corrector was designed using a low index, low dispersion glass, Schott FK54. Using this single element corrector, the

5

entire field of the larger candidate CCD is diffraction limited over the entire wavelength range of Silicon sensors. The best focus is now the same with field angle. The corrector element should not be very expensive to make as it has only spherical surfaces and is of modest diameter, compared to the Schmidt-Cassegrain.

Other Parameters Affecting Resolution

The MTF of the final imaging system is not limited by the telescope design and the diffraction limit of the aperture. Other sources of degradation were quantified by the MTF function:

CCD Imager Pixel Size Effects
The finite size of a CCD pixel acts as a spatial low pass filter as it integrates and averages image energy over its surface. For a square pixel CCD of width "w" with uniform sensitivity over its area, the geometric based MTF as a function of spatial frequency, v, is:

$$MTF_{geo\_pixel} = \sin(\pi\, v\, w) / (\pi\, v\, w),$$

For: w = 0.007 millimeters
      v = 69 cycles/millimeter,

$$MTF_{geo\_pixel} = 0.658$$

Gaussian Probability Distribution, Line-of-Sight Jitter
Jitter of the telescope line-of-sight spreads the image energy spatially during an integration time of the CCD imager and therefore acts as a low pass filter. For a standard deviation random jitter of s radians during an exposure, the MTF was shown to be:

$$MTF_{jitter} = \exp(-2\, \pi^2\, (s \cdot EFL)^2\, v^2),$$

for:

          $s = 2.01 \cdot 10^{-6}$ radians, the pointing stability requirement (1 sigma),
          EFL = 2159 millimeters,
          v = 69 cycles/millimeter

$$MTF_{jitter} = 0.170$$

Linear Image Motion
Linear image motion creates a one-dimensional blur in the direction of the motion during an integration time and therefore acts as a low pass filter in the direction of the blur. For pushbroom type scanning, a linear array is scanned across the image by the vehicle motion, much like a fax machine. Hence, this motion is necessary to yield a two-dimensional image and its subsequent blur is inescapable. It is possible to compensate for this blur by decreasing the sample spacing between line images. For example, if the line array is moved only half a pixel width instead of a full pixel width for each line image scan, the image is built-up with twice the resolution along the motion direction, compensating for the increased blur.

To achieve a sequence of images and enhance the information gathering capability of the satellite, a nadir pointed telescope could take a sequence of images, shuttering the CCD to control the exposure and the blur. The resulting MTF from linear motion can be calculated by:

$$MTF_{linear\ motion} = \sin(\pi\, v\, m\, t) / (\pi\, v\, m\, t),$$

where:
v is spatial frequency in cycles/millimeter,
m is image motion in millimeters/sec on the focal plane, t is integration time in seconds and:

$$m = velocity(mm/sec) \cdot EFL(mm.) / altitude(mm.)$$

for a circular orbit:
velocity(km/s) = [$(9.8 \cdot 10^{-3}$ km/s) $\cdot$ $(6370$ km$)^2$ / (6370 km + altitude(km.)) $]^{0.5}$

where:
          6370 km. is the radius of the earth.
          9.8 m/s is acceleration due to gravity.

Other quantifiable effects include: atmospheric refractive turbulence, residual telescope fabrication errors, scattering in the atmosphere, charge migration between CCD pixels, and bandwidths of analog amplifiers in the CCD readout circuitry. These effects are dependent on the time-of-day, the particular telescope and CCD used and the readout rate of the CCD.

We can multiply the MTF's of the calculated degradation to yield a system MTF and include additional terms as they are determined or calculated. For the designed telescope, with 7 micron pixels, 0.5 microradian jitter, and half-pixel image motion, we get a system MTF of approximately 0.2. This system MTF was used to simulate the imaging of the satellite by taking a known scale reference image, 2-D Fourier transform of it, multiplying the image spectrum by the MTF, then inverse transforming the product. The resulting image was then compared to the reference image for various design parameter trades.

Pointing and Control

A proposed pointing scenario for the imaging slew is as follows. The satellite is pitched forward from a nominal nadir-pointing attitude to predetermined new attitude, and then pitched in reverse during imaging to

6

reduce the line-of-sight transverse velocity at the surface of the earth. Without this counter motion, the satellite velocity over an integration period will result in too much blur of the picture. The amount by which the satellite must be initially pitched forward in preparation for the imaging slew depends upon the amount of time required to settle out initial pitch slew transients once the imaging slew begins. The time requirement, in turn, depends upon the controller bandwidth. A higher controller bandwidth will result in transients subsiding quicker but will result in a greater response to sensor noise.

Figure 1 shows the satellite imaging geometry assumed for this analysis [2] with an altitude of 408 km.
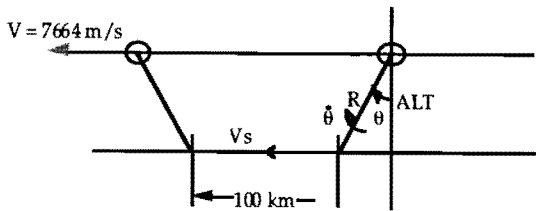
Figure 1. Satellite imaging geometry (flat earth assumption)

From this geometry the required ground speed traced out by the satellite LOS is 2353 m/s. For a swath length of 100 km, the imaging time is 42.5 secs. In this time, the satellite travels a distance 326 km. The look ahead angle is given by:

$$\theta = \tan^{-1}\frac{(325.72-100)/2}{408}$$
$$= \sim 15.5°$$

Actual imaging begins at a look-ahead angle of ~15.5° with a stabilized LOS rate of ~ .75°/s. The important point here is that the LOS rate must be stabilized so that the image advances 1 m in the read-out time of 0.425 ms. In order to stabilize the LOS rate, the maneuver must begin before the actual imaging at a look-ahead angle greater than 15.5°. The required initial angle for the slew maneuver will depend upon the transient response (and, therefore, the bandwidth) of the controller.

The major disturbance torques acting on the satellite are due to the following [2]:

Gravity gradient torque about the pitch (y-) axis is given by:

$$M_G = 3\omega_o^2 (I_{zz}-I_{xx}) \sin\theta \cos\theta$$

where w_o is the orbit rate.

Aerodynamic torque is given by:

$$M_A = C_D \, q \, S \, l$$

where
C_D : drag coefficient
q : dynamic pressure
S : satellite projected area
l : distance between center-of-pressure and center-of-mass.

Residual magnetic dipole moment is given by:

$$M_M = 10^{-7}\frac{2MD}{r^3} \text{(polar orbit)}$$

where
M : magnetic moment (8×10^{25} emu at Earth)
D : residual dipole (pole cm)
r : orbit radius (cm)

The disturbance torques were estimated to be as follows:

M_G = $-.275\times10^{-6}$ Nm per degree

M_A = $\pm1.6\times10^{-6}$ Nm (moment arm = ±1cm)

M_M = $\pm1.1\times10^{-5}$ Nm (±200 pole cm residual dipole)

It is interesting that the torque due to a residual magnetic dipole may be an order of magnitude greater than either the gravity gradient or aerodynamic torque. This suggests that it should be compensated using the torque rods which are otherwise required for orbit acquisition and momentum desaturation. It should be possible to reduce the disturbance torque due to the residual magnetic dipole by an order of magnitude. Compensation is assumed in the following analysis (i.e., the residual dipole torque is taken as $\pm1\times10^{-6}$ Nm).

INS/GPS Role

Miniature INS/GPS systems are currently under development. The system typically contains a Micromechanical Inertial Measurement Unit (MMIMU) comprising three orthogonal micromechanical accelerometer instruments and three orthogonal micromechanical gyro instruments with individual conditioning electronics and high-resolution digital output quantizers. The system also contains a GPS receiver as well as a guidance and navigation processor. This entire system is miniaturized further using low power mixed signal CMOS ASICs, high-performance bump bonding techniques, shared/multiplexed electronics functions and advanced

7

high-density packaging. A single clock, voltage reference, A/D converter, and DSP are used to service the micromechanical INS/GPS system, resulting in a compact, low-power, multisensor, multi-axis system. The complete INS/GPS system occupies less volume than a hockey puck. Power dissipation is minimized both through the use of low power CMOS and also by using power conserving sleep modes.

GPS Role

The determination of attitude using GPS is based upon the carrier phase difference between two antenna tracking the same satellite. GPS provides position with accuracy on the order of a few meters, and provides a highly reliable technique for providing attitude using interferometry techniques. Attitude determination using GPS is based on a simple geometric principle: two distinct points uniquely define a line and three noncolinear points define a plane. Treating GPS antennas with known relative positions as the noncolinear points, the orientation of the plane in which they reside can be determined, as well as the orientation of the antennas within the plane. This is achieved by using the differences in phase of the incoming GPS carrier signal between the antennas, hence the term "GPS interferometry".

The ability to determine the translation and rotation state of a satellite is dependent on the number of GPS satellites in view and the resulting measurement geometry. Since the GPS system was designed for "Earth-bound" users, the GPS satellite radiation signal is directed toward Earth. Satellites at altitudes up to approximately 1000 km will generally find 10 or more satellites "in view". At higher altitude, the user may be outside the main radiation beam of some GPS satellites. At altitudes above roughly 3000 km, the number "in view" may frequently drop below 4. Although 4 satellites in view is generally considered the minimum set to solve for both the three components of position and the user clock bias, studies have shown that acquisition of a single GPS satellite can be adequate to maintain orbit accuracy. Thus, satellites in either high altitude or highly elliptic orbits can maintain accurate position information.

Micromechanical IMU Role

In a small satellite, the micro-mechanical IMU data can be blended optimally with the GPS data, thereby taking advantage of the IMU's ability to measure high-frequency dynamics and the GPS's ability to bound the error growth due to gyro drift.

A small satellite should have attitude determination capability at any orientation in space. The ability to determine attitude from a "cold start" without any prior knowledge is also important. Furthermore, the ability to measure rotation rates will be crucial to achieving stable conditions at any desired attitude. The micromechanical IMU can play a major role in alleviating these problems.

The ability to instantaneously measure via GPS all components of vehicle attitude can place severe requirements on spacecraft geometry and antenna mounting to ensure observability. Antennas must be mounted such that both antennas making up a baseline can observe the same satellite without masking problems. Furthermore, this condition must be met for more than one baseline and satellite. Using the micromechanical IMU (or gyro package) as a reference permits us to bridge small gaps in interferometer coverage in both a spatial and temporal sense. This can reduce the number of antennas required and mitigate problems arising from field-of-view masking due to factors such as solar arrays or other instrumentation.

Two other key roles for the IMU are control feedback for both rotational and translation maneuvers. First, attitude pointing and stabilization requires high-speed, low-noise measurements for effective control. GPS measurements alone (without an IMU) will be too noisy for effective attitude control if antenna baselines are short. Second, translation maneuvers can be provided with instant 3-axis measurement of Δv maneuvers via the IMU to perform orbit placement or adjustment. GPS has the ability to measure velocity changes very precisely via carrier tracking, and therefore could be used in place of the IMU accelerometers. Use of the IMU is more straightforward and eliminates antenna masking and satellite observability concerns.

Attitude Determination Analysis

Attitude determination depends upon both GPS and gyro attitude sensors for precise attitude knowledge and as a reference for the attitude control system and imaging slew maneuver. A Kalman filter combines the GPS and gyro measurements to provide an optimal estimate of satellite attitude and to calibrate the rate gyros.

The image swath dimensions for the present application are 100 km down-track and 7 km cross-track. In order to avoid missing the primary target, the requirement for the radius of the pointing error circle in the middle of the image swath was set at 1.5 km (3-sigma). The total pointing error contains contributions from the GPS orbital position error of 100m (1-sigma), the satellite attitude knowledge error, and the pointing control error. For this analysis, the attitude knowledge error and attitude control error are assumed to contribute equally. Furthermore, the attitude knowledge must be retained during the imaging slew maneuver. This may be a difficult

8

requirement to meet given that the satellite is slewing over a large angular range at nearly 1°/sec. GPS satellite visibility and switching of satellites could conceivably degrade attitude knowledge during the slew. Alternatively, relying upon the gyros through the imaging slew to retain attitude knowledge accuracy results in the following requirements for gyro bias and scale factor uncertainty:

The GPS attitude error is modeled as a 1st-order Gauss-Markov process. This model is based upon ground testing of a satellite mock-up. The GPS receiver used in that test was the Trimble TANS Vector and the antenna baselength was approximately 50 cm. Most of the error is thought to be contributed by the effects of multipath reflections. The correlation time observed in the ground tests was approximately 100 s and the GPS error magnitude was approximately 0.28 deg about the yaw axis (along the nadir direction). The error magnitudes about the pitch and roll axes were slightly less. The nominal values used in this simulation were 0.28 deg for magnitude, with a correlation time of 100 s.

A covariance simulation of gyro and GPS attitude measurements combined in an extended Kalman filter was used to predict satellite attitude determination performance as a function of gyro error characteristics. Only a single-axis analysis was performed but the results should be quite representative of a three-axes implementation. The nominal performance was predicted for a range of gyro performance error parameters. Results of the analysis indicate a gyro bias drift on the order of 0.01 deg/hr is required to meet the pointing requirement of 1 milliradian.

Model Based Kalman Filter

As part of a continued effort to enable micromechanical gyroscopes for satellite applications, work was initiated on a program to improve traditional attitude estimation filtering algorithms by including vehicle dynamics in a Kalman filter design. Typically, the excellent performance of high-cost gyros saw little benefit from the blending of gyro rate data with vehicle dynamics information. However, current trends in small satellite and other aerospace vehicle design [5,6] favor using lower cost, lighter weight instruments, such as micromechanical gyros. Attitude filters which utilize micromechanical gyros as attitude sensors can often significantly improve their performance when vehicle dynamics data is incorporated into the filtering algorithm and used to reduce uncertainty in gyro error states, such as gyro bias drift.

The approach taken as part of an ongoing research project, is to develop a small satellite nonlinear dynamics simulation, linearize the dynamics model about a gravity-gradient stable position, and design a continuous linear time-invariant steady-state Kalman filter about this model, incorporating measurement information from micromechanical gyros and GPS attitude sensors. This allows us to demonstrate the feasibility of augmenting the filter with dynamics information to achieve improved attitude filter performance. Our current focus is on expanding the design to a linear discrete filter, to allow differing sensor update rates, and then to an extended Kalman filter, to allow attitude estimation at any spacecraft orientation. Additionally, the capabilities of the system will be expanded with the addition of improved space environment models, better gyro error and GPS error (e.g., multipath) models, and the introduction of some robust estimation techniques developed at Draper Laboratory [7,8,9,10] to desensitize filter performance to vehicle modeling errors.

Results for the continuous linear time-invariant steady state filter show marked improvement with the use of vehicle dynamics data. For a small satellite with GPS attitude data accurate to 0.3 deg (1-sigma) and gyro rate data corrupted by drift with 0.05 deg/rt-hr angle random walk and 10 deg/hr (over 10 hrs) drift, the standard deviation of the single axis attitude estimation error was reduced from 0.25 deg. to 0.03 deg. with vehicle model information. These performance figures were gathered from sample statistics of the data shown below over a ten hour simulation period, during which the satellite was oscillating about a gravity gradient stable position.

Since GPS measurements were simulated as corrupted only by 0.3 deg. (1-sigma) white noise, some degradation in performance is expected with more realistic multipath error models. However, the distinct improvement in attitude estimation error shown with the model based filter is still expected to be present in cases with more accurately simulated multipath error.

9
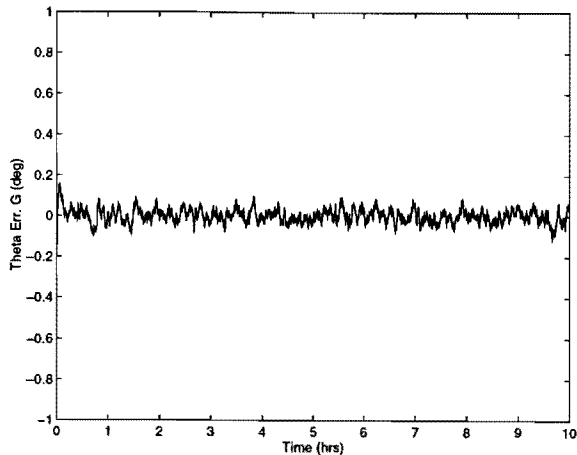
Fig. 1: Error in Angle Estimate with Vehicle Model-Based Filter
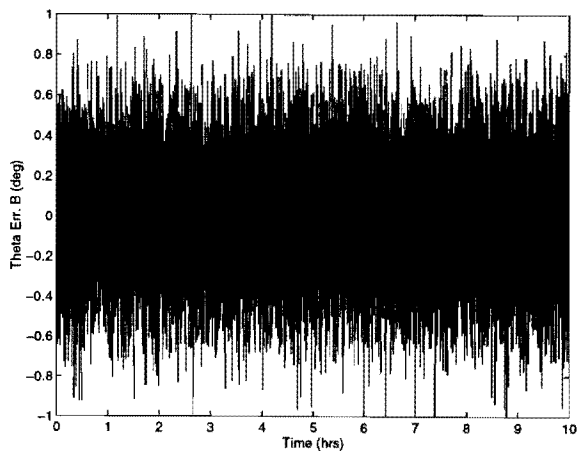
Fig. 2: Error in Angle Estimate Without Vehicle Model-based Filter

The model-based filter also provides the capability to sustain adequate attitude knowledge during GPS blackout periods. Similar simulation results show that the attitude estimator with vehicle dynamics model information is able to maintain attitude knowledge to within several degrees hours after the loss of direct attitude data from GPS. However, the attitude solution of the traditional filter without the advantage of vehicle dynamics model information quickly diverges.

Ground Test Experiment

The MicroSat ground testbed assembly consists of the optical pointing system, including the telescope, field corrector lenses, camera, and spacers, reaction wheels with drive electronics, inertial instruments, control

processor, and the support structure. The optical pointing system is mounted on a single axis rotary air bearing, with the option of installing small-angle flexural pivots for the across-track axis. The air bearing in turn is mounted on a 35.6 cm (14 in.) optical grade granite table. Off board is a Pentium based PC used for controlling the experiment, algorithm development, image storage, and data display. The resolution targets are located 52 meters away in the longest continuous hallway at the Laboratory with Halogen lights providing a combined luminosity that approaches sunlight on a clear day.

The optical system is a Draper designed, custom fabricated 37 centimeter Ritchey-Chretian Cassegrain telescope with a 5K element line array CCD. The telescope has a mass of 11.36 kg, is 76 cm in length with a focal length of 3.1 meter and an F# of 8.5. This calculation is done at three different field angles: on-axis and off-axis field angles corresponding to the edge corner of the same two candidate CCD's. At the sampling spatial frequency of 69 line-pairs per millimeter, the MTF design performance on-axis and at the smaller CCD corner edge is diffraction limited and about 0.36. We see that the performance at the larger CCD corner edge is low, this is due mostly to field curvature of the focal surface and astigmatism. The field angle dependent image defects of this telescope are correctable using a weak negative meniscus lens in-front of the CCD. A field corrector assembly was fabricated using a low index, low dispersion glass, Schott FK54. Using this single element corrector, the entire field of the larger candidate CCD is diffraction limited over the entire wavelength range of Silicon sensors.
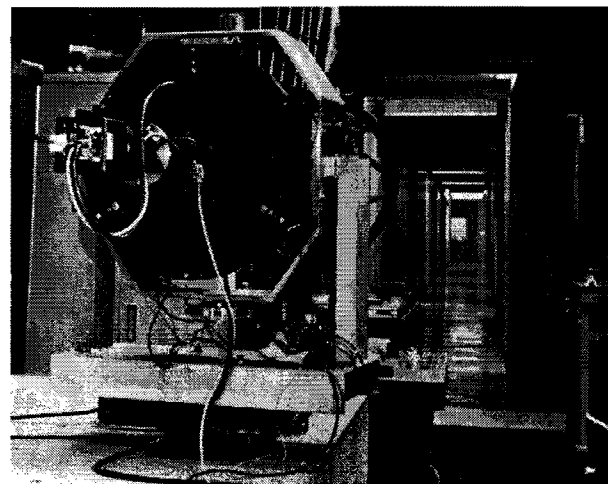
A reaction wheel uses a rotary inertia to impart an angular momentum on the system. Due to conservation of angular momentum, an equal and

10

opposite angular momentum is imparted on the satellite when the wheel inertia is spun. This reaction angular momentum causes rotation of the satellite. The ground test reaction wheels were designed and built for this project, and consist of electronics, rotor, bearings, motor, and housing. The drive electronics is capable of operating in a velocity mode or a torque mode. Measurement of rotation rate is accomplished by reading the integral Hall sensors. These send an analog signal to the A/D converter in the data acquisition and control module.

A precise knowledge of the platform speed and position is necessary for closed loop control. Thus, a central component of the ground test is the gyro. The unit selected is a Systron Donner QRS11. The bias and noise characteristics of the gyro were measured before integration. Gyro noise sampled at 50 Hz for 60 minutes and is analytically determined to be "white noise" uncorrelated, random fluctuations.

A slew maneuver that reconstructs the pointing scenario is commanded through the embedded processor. Currently the ground test consists of single axis (azimuth) control. The control of the reaction wheel allows the optics array to slew in the azimuth axis. This is necessary because the Dalsa linear CCD consists of a line of 4096 7 micron x 7 micron photosensors. As the MicroSat sweeps across the target each photosensors senses a pixel of the image and immediately delivers that pixel to a Raptor video board. Meanwhile, the MicroSat has moved a few milliradians and the photosensor senses a new pixel. The integral of all these linear images produces a 2 dimensional picture of the target.

The Ground Sampling Distance (GSD) of an image was determined by examining a resolution chart, comprised of the USAF 1951 Test Pattern. The chart is used to determine line spacings that subtend a small enough angle to test the limit of resolution of the telescope. By deciding which square of three lines is the smallest discernible pair, it is possible to gauge the GSD of the system. For a single axis, closed loop slew, the equivalent ground resolution was determined to be 1.4 meter.

Conclusions

The MicroSat Project has been an internally funded project to investigate and develop technologies to support, advance, and contribute to the continually increasing demand for small satellites. The MicroSat Project is a single, inter-departmental project focusing Draper technologies, design approaches, and expertise toward developing a unique system-based solution for precision pointing applications in small, lightweight satellites. Although a point-design was selected to focus the project's efforts, the central spacecraft design is applicable to many military and scientific remote-sensing missions requiring precision pointing and stabilization. The MicroSat Project developed a complete system design for a visible imaging microsatellite capable of returning images of one meter class resolution and demonstrated the optics and pointing subsystem in a ground test imaging experiment.

References

[1] Metzinger, R., "Quick Look Summary of a 31:2 Orbit for MicroSat," Draper Memo E21-95-956, 10 November 1995.

[2] Madden, P., "Requirements for Microsat Slew Control During Imaging," Draper Memo E43-95-107, 1 May 1995.

[3] Madden, P., "Microsst On-Orbit Control Analysis," Draper Memo E43-95-163, 13 July 1995.

[4] Cappiello, G., "MicroSat Imaging System Preliminary Layout and Design Consideration," Draper Memo ETB-94-484, 20 December 1994.

[5] Koifman, M., and Merhav, S., "Autonomously Aided Strapdown Attitude Reference System", *Journal of Guidance, Control and Dynamics,*, 1991.

[6] Merhav, S., *Aerospace Sensor Systems and Applications,* Springer-Verlag, 1996, Chapter 9, pp. 423-439.

[7] Mangoubi, R., "Robust Esimation and Failure Detection for Linear Systems," PhD Dissertation, M.I.T. Department of Aeronautics and Astronautics, 1995, and Draper Laboratory Report CSDL-T-1237.

[8] Mangoubi, R., Appleby, B., Verghese, G., "Robust Estimation for Discrete-Time Linear Systems," *Proc. of the American Control Conference,* pp. 656-661, May 1994.

[9] Jaquemont, C., "Aircraft Attitude Determination Using Robust Estimation," M.S. Thesis, M.I.T. Department of Aeronautics and Astronautics, 1997.

[10] Agustin, R., Mangoubi, R., Hain, R., and Adams, N., "Robust Thrust Estimation for Aerospace Vehicle Reaction Control Systems," *Proc. of the American Control Conference,* June 1997.

11